18TH WORLD CONFERENCE ON EARTHQUAKE ENGINEERING
WCEE2024
MILAN

MILAN, ITALY
30TH JUNE - 5TH JULY 2024

www.wcee2024.it

PB-LOSS: A FUTURE CANDIDATE FOR SEISMIC RISK CLASSIFICATION GUIDELINES

G.J. O'Reilly[1] & A.M.B. Nafeh[1]

[1]Centre for Training and Research on Reduction of Seismic Risk (ROSE Centre), Scuola Universitaria Superiore IUSS Pavia, Italy, gerard.oreilly@iusspavia.it

Abstract: *Loss assessment is becoming an increasingly common component in the seismic performance classification of existing structures, with different approaches available. The most notable is the component-based approach implemented within the FEMA P-58 guidelines. Additionally, practitioners must be provided with tools to conduct building-specific loss assessments in a simple and expedited manner without compromising accuracy. The component-based approach may thus be computationally expensive regarding time and resources required, such as numerical modelling, ground-motion selection, non-linear time-history analysis and post-processing of results. To this end, this study presents a simplified alternative to computationally expensive assessments via a pushover-based approach to estimate economic losses, denoted as "PB-Loss", intended for code-based applications. The approach implements simplified procedures to quantify seismic hazard, vulnerability and risk. The most notable component of the proposed pushover-based approach is the implementation of storey-loss functions (SLFs). SLFs simplify the process of estimating repair costs for a given building typology by avoiding the need for numerous steps involving the estimation of damage states and repair costs for each individual damageable component, resulting in reduced computational effort. To demonstrate the effectiveness of the proposed method, PB-Loss was evaluated via a comparison with other simplified procedures currently in use for seismic risk classification. This study highlighted that, when compared to the more rigorous component-based approach, PB-Loss demonstrates high levels of accuracy and robustness, highlighting its potential to be adopted in future codes and guidelines and rendering it a strong candidate for use in practical applications.*

1. Introduction

Despite the emergence of various methodologies for assessing seismic risk and loss in recent years, there remains a need to provide practitioners and engineers with simplified tools to conduct building-specific loss assessments. These are essential to facilitate more informed decision-making at the practitioner level. One key reason for this need is that comprehensive probabilistic methods can seem overly intricate and detailed for practical decision-making. For example, the Pacific Earthquake Engineering Research Center's Performance-Based Earthquake Engineering (PEER-PBEE) framework (Cornell and Krawinkler, 2000; Krawinkler and Miranda, 2004) evaluates the overall performance of a specific building using a fully probabilistic approach that takes into account uncertainties related to hazard, structural response, damage estimation, and economic loss calculation. However, due to its probabilistic and computationally intensive nature, it remains mainly favoured within the academic community and specialised studies and reports, such as FEMA P-58 (FEMA, 2012b) and the CNR guidelines (CNR, 2014). One simply needs to examine the component-based approach of FEMA P-58 (FEMA, 2012b) to understand the level of detail required, such as numerical models detailed enough to capture all possible inelastic mechanisms, ground motion selection for non-linear time history analyses, damageable inventories with quantities, fragility functions and expected repair costs for every single damageable element, among other steps. In Europe, various studies (Del Vecchio et al., 2018) have consistently emphasised the need to develop alternative methods that better reflect the local context, while others (Silva et al., 2020) have suggested ways to adapt the FEMA P-58 database, for example. This need is further underlined by the Italian government's decision (Ministero delle Infrastrutture e dei Trasporti, 2017), known as the Italian guidelines for seismic risk classification of constructions (Cosenza et al.,

2018) to employ seismic loss estimates as a means to quantify seismic risk and adopt it as a parameter to offer financial incentives to building owners willing to upgrade and retrofit.

To address these needs, this study outlines a simple and practical framework to estimate direct economic losses in structures based on static pushover (SPO) analysis results. It exploits the storey-loss function (SLF)-based concept by Ramirez and Miranda (2009) as an alternative to component-based loss assessment. As such, a generic set of SLFs, previously derived by Nafeh and O'Reilly (2023) for infilled RC building typologies representative of those found in Italy is formalised into a pushover-based seismic loss assessment methodology, termed *PB-Loss* herein. Its accuracy and improvement compared to adopted national guidelines are appraised.

2. PB-Loss methodology

The *PB-Loss* methodology builds upon previous research (Nafeh and O'Reilly, 2023), denoted *PB-Risk* that evaluates the earthquake performance of a single building using a pushover analysis to estimate the structural vulnerability. *PB-Loss* expands this by offering straightforward means to estimate financial losses expected in a building solely through a pushover analysis. After characterising the seismic hazard and vulnerability components, the seismic losses can be calculated using a generalised set of SLFs designed for infilled RC typologies. This section provides an overview of the general steps involved in the proposed *PB-Loss* framework, which incorporates four primary modules, namely: 1) hazard, 2) vulnerability, 3) risk and 4) loss.

2.1. Seismic hazard

a) Perform probabilistic seismic hazard assessment (PSHA) to determine the annual rate of exceeding a specified ground motion intensity level, denoted as $H(IM)$, or alternatively, use the outcome from a suitable seismic hazard study. In *PB-Loss*, $H(IM)$ should be characterised for two intensity measures: the peak ground acceleration (PGA) and the average spectral acceleration, $Sa_{avg}(T^*)$, where T^* is the anchoring period. The calculation of Sa_{avg} adheres to the definition provided by Eads *et al.* (2015) with the modifications proposed by O'Reilly (2021) for the associated period range:

$$Sa_{avg} = \left(\prod_{i=1}^{N} Sa(c_i T^*)\right)^{1/N} \quad (1)$$

where c_i represent N=10 number coefficients in the range of 0.2 and 3.0 to account for period-elongation effects in non-ductile infilled RC frame buildings;

b) From each hazard curve (i.e., PGA and $Sa_{avg}(T^*)$), determine the ground motion intensities, *im*, associated with the return periods, T_R, specified by the Italian national code (NTC18) (NTC, 2018), or any other nationally governing guideline. Their annual rates of exceedance, $H(IM)$, are calculated as the inverse of the return periods where $H(IM) = 1/T_R$. NTC18 adopts the four return periods reported in Table 1.

Table 1: NTC18 return periods for residential buildings

Limit State	Return Period, T_R [years]	Annual Rate of Exceedance, $H(IM) = 1/T_R$
Operational Limit State (OLS)	30	0.033
Damage Limitation Limit State (DLLS)	50	0.020
Life-Safety Limit State (LSLS)	475	0.0021
Collapse Prevention Limit State (CPLS)	975	0.0010

c) Fit a second-order approximation to the IM = $Sa_{avg}(T^*)$ hazard curve, illustrated in Figure 1 where $H(IM)$ denotes the mean annual rates of exceeding an *IM* value described by:

$$H(IM) = k_0 \exp\left[-k_2 ln^2(IM) - k_1 \ln(IM)\right] \quad (2)$$

where k_0, k_1 and k_2 are coefficients describing the second-order hazard fitting and can be identified using the approach and tools outlined in Shahnazaryan and O'Reilly (2023).

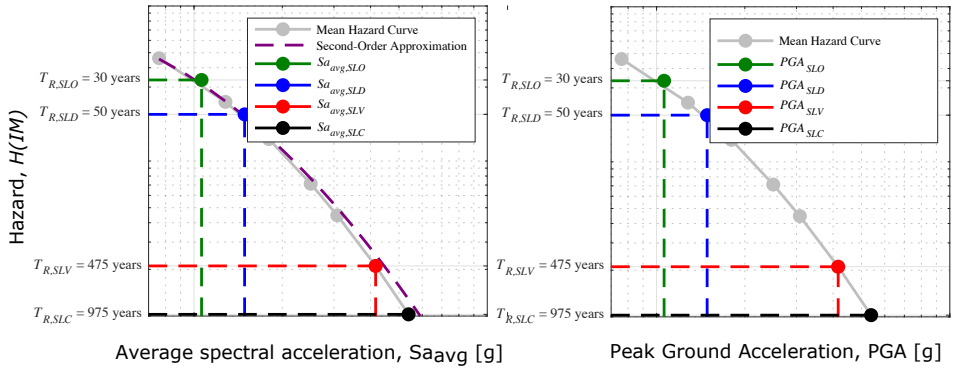

Figure 1: Sa_{avg} and PGA hazard curves expressed in terms of the annual exceedance rates, H(IM), and the intensity measure levels, im, at the identified NTC2018 code-based return periods, T_R

2.2. Seismic vulnerability

a) Build a sufficiently detailed numerical model of the structure accounting for all possible failure modes and inelastic mechanisms;

b) Perform a modal analysis to characterise the normalised first-mode shape, $\Phi_{1,i}$, at each floor *i*;

c) Perform a SPO analysis in both principal directions of the building to characterise the lateral response in terms of base shear, V_b, and roof displacement, Δ_{roof};

d) Multi-linearise the SPO curve to indicate the onset and end of each response branch (i.e., elastic, hardening, post-capping or softening and residual strength plateau) as illustrated in Figure 2;

e) Identify the equivalent single-degree-of-freedom (SDOF) properties, expressed in terms of equivalent base shear, V_b^*, and displacement, Δ^*, as follows:

$$V_b^* = \frac{V_b}{\Gamma} \tag{3}$$

$$\Delta^* = \frac{\Delta_{roof}}{\Gamma} \tag{4}$$

$$\Gamma = \frac{\sum_i m_i \Phi_{1,i}}{\sum_i m_i \Phi_{1,i}^2} \tag{5}$$

where Γ is the first-mode transformation factor computed via Equation (5) assuming a first-mode based non-torsional behaviour of the building, m^* and T^* are the effective mass and period of the equivalent SDOF system; m_i is the mass at floor *i* of the multi-degree-of-freedom (MDOF) system;

f) Using the response evaluation tool for infilled RC frames (O'Reilly and Nafeh, 2021; Nafeh and O'Reilly, 2022) (available at: https://github.com/gerardjoreilly/Infilled-RC-Building-Response-Estimation), the seismic demand-intensity model is calculated for the structure's equivalent SDOF in both principal directions of the building. It is expressed as a dynamic strength ratio, ρ, for a given ductility demand, μ, via the ρ-μ-T relationships. It estimates both the collapse and non-collapse performance of the equivalent SDOF structure (Figure 2);

g) The median intensity required for the MDOF system to exceed a given ductility demand is computed from the tool's output value of $\hat{\rho}$ as:

$$\widehat{Sa}_{avg} = \hat{\rho} Sa_y^* \Gamma \tag{6}$$

$$Sa_y^* = \frac{4\pi\Delta_y^*}{T^{*2} g} = \frac{V_{b,y}^*}{m^* g} \tag{7}$$

where Sa_y^* is the yield spectral acceleration of the equivalent SDOF system indicated in Equation 7 and $V_{b,y}^*$ and Δ_y^* are the base shear and displacement at the yield point of the equivalent SDOF system;

h) For collapse, the median seismic collapse intensity, $\widehat{Sa}_{avg,C}$, and the associated dispersion, β_C are identified directly by the response estimation tool.

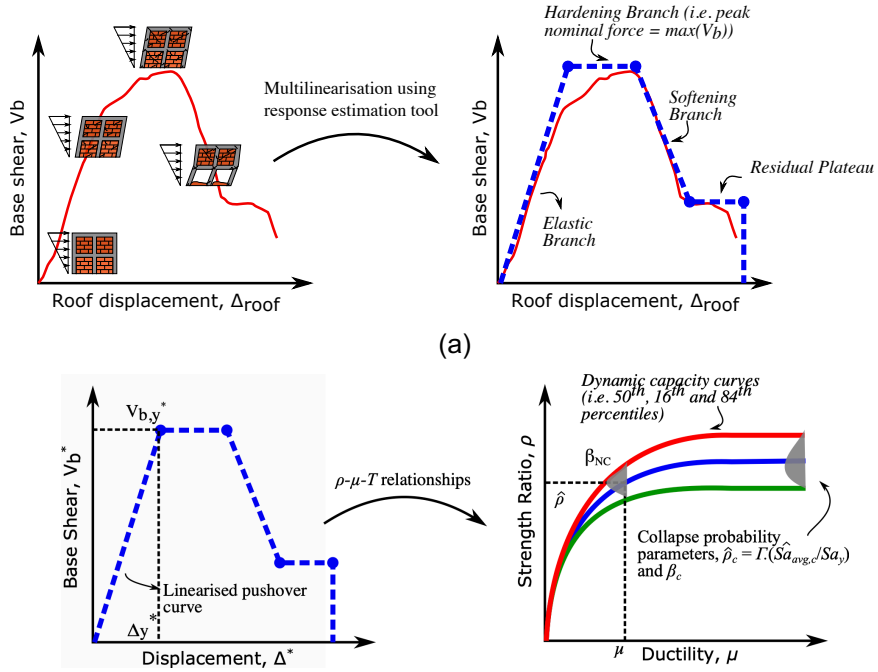

Figure 2: (a) Multi-linearisation of SPO curve based on onset and end of response branches, and (b) the estimation of dynamic response via the ρ-μ-T relationships

2.3. Seismic demand estimation

While the previous section discussed characterising the response of an equivalent SDOF system, the seismic demand in the actual MDOF structure is characterised via peak storey drift (PSD) and peak floor acceleration (PFA) quantities. The PSD demands are a notable contributor to the damage of drift-sensitive structural and non-structural components whereas PFA demands contribute significantly to the damage in acceleration-sensitive non-structural components. Moreover, another component of seismic loss assessment is the residual PSD (RPSD) remaining in the structure once the shaking has stopped. The influence of residual drifts is related to the possibility of a building requiring demolition due to excessive permanent lateral deformation. In the following sub-sections, simplified approaches to estimate PSD, PFA and RPSD quantities are described.

2.3.1. Peak storey drifts

a) For each *im* value, estimate the roof displacement demand $\Delta_{roof,im}$ for non-collapse via interpolation of the dynamic capacity curves obtained from the response estimation tool (Figure 3);

$$\Delta_{roof,im} = \mu_{im}\Delta_y^*\Gamma \tag{8}$$

b) Using a first-mode approximation of the building response, identify the PSD demand profile in each direction of the building at each *im* (Figure 3):

$$\Delta_{i,im} = \Phi_{1,i}\Delta_{roof,im} \tag{9}$$

$$\theta_{i,im} = \frac{\Delta_{i+1,im} - \Delta_{i,im}}{h_i} \tag{10}$$

where $\Delta_{i,im}$ is the displacement at floor *i* for a particular *im*; $\Delta_{roof,im}$ is the roof displacement at a given *im* value of the MDOF system; μ_{im} is the ductility at a given *im* value (i.e., $\mu_{im} = {\Delta_{roof,im}}/{\Delta_{y,roof}}$); h_i is the height of storey *i*, and $\theta_{i,im}$ is the drift of storey *i* at the given *im*.

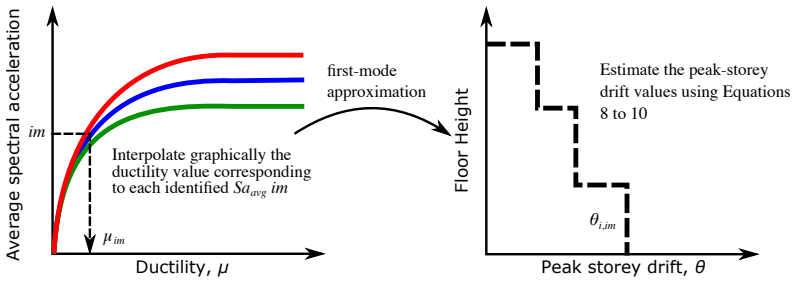

Figure 3: First-mode-based approximation to estimate the peak-storey drift demand profiles

2.3.2. Peak floor accelerations

The deformation-dependent peak floor estimation method highlighted by Muho *et al.* (2021) is adopted in *PB-Loss* due to its simplicity and the robustness of the empirical deformation-acceleration relationships, as investigated by Nafeh and O'Reilly (2023) for the case of non-ductile frames with infills. As such, the user must:

a) Select an approximate shape for the acceleration profile based on the number of storeys, as shown in Figure 4;

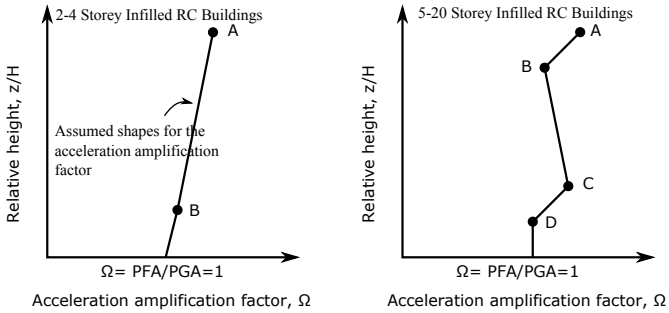

Figure 4: Approximation of the acceleration amplification factor profiles for 2 to 4-storey (left) and 5-20 storey (right) infilled RC buildings (adapted from Muho et al. (2021)*)*

b) The acceleration amplification factor, $\Omega_{i,im}$, defined as the ratio between the PFA at floor *i* and the PGA for a given intensity, *im,* can be estimated as:

$$\Omega_{i,im} = \frac{PFA_{i,im}}{PGA_{im}} = a_1 \theta_{i,im}^{a_2} T^{a_3} \left(\frac{E_2}{E_1}\right)^{a_4} t^{a_5} \quad (11)$$

where a_1, a_2, a_3, a_4, a_5 are calibrated parameters (Table 2) for each point on the expected shape of the acceleration amplification factor; $\theta_{,im}$ is the estimated PSD (in %) intensity *im* computed via Equation 10; *T* is the fundamental period of the structure (in s); E_1 and E_2 are the horizontal and vertical moduli of elasticity of infill panels (in MPa), respectively; *t* is the thickness of the infill panels (in metres).

Table 2: Empirical parameters for the quantification of the acceleration amplification factor of 2-20 storey infilled RC frame structures (adapted from Muho et al. (2021)*)*

Profile	**2-4 storeys**					**5-20 storeys**				
points	**a_1**	**a_2**	**a_3**	**a_4**	**a_5**	**a_1**	**a_2**	**a_3**	**a_4**	**a_5**
A	0.308	-0.460	0.055	-0.168	0.259	0.259	-0.438	-0.256	-0.270	0.196
B	0.645	-0.178	-0.148	-0.090	0.136	0.161	-0.463	-0.336	-0.291	0.145
C	-					0.708	-0.145	-0.206	-0.103	0.087
D	-					1.159	-0.027	-0.170	-0.048	0.076

2.3.3. Residual peak storey drifts

The FEMA P-58 methodologies (FEMA, 2012a) approximation was adopted to estimate the RPSD due to its independence of ground-motion characteristics and its straightforward application. The method assumes the following conditions are met: building response along each principal direction is independent; the building is

regular; PSD does not exceed four times the drift at yield; storey drifts are less than 4% beyond which geometric non-linearity (i.e., P-Δ) effects tend to become dominant. Equation 12 describes the approximation:

$$\begin{aligned} \theta_{res,i,im} &= 0 && if\ \theta_{i,im} \leq \theta_y \\ \theta_{res,i,im} &= 0.3(\theta_{i,im} - \theta_y) && if\ \theta_y < \theta_{i,im} \leq 4\theta_y \\ \theta_{res,i,im} &= (\theta_{i,im} - 3\theta_y) && if\ 4\theta_y < \theta_{i,im} \end{aligned} \quad (12)$$

where $\theta_{res,i,im}$ is the estimated RPSD at a given *im* at floor *i*; $\theta_{i,im}$ is the estimated PSD at floor *i* (from Equation 10); θ_y is the drift at yield determined using Equations 9 and 10. Naturally, the estimation of the RPSD must be carried out in both principal directions, where separate pushover analyses are carried out. However, one limitation of the proposed approach is that for the infilled RC buildings case, if shear failure is to occur at the top of the columns, a global collapse mechanism could be triggered. The latter effect cannot be captured checking the drift or residual drift since it has a low drift demand (even lower residual drift).

2.4. Collapse risk estimation

Figure 1 previously reported four non-collapse intensities, *im,* to be evaluated in *PB-Loss*, although many more intermediate intensities could also be adopted. However, for the case of collapse, where the mean annual frequency of collapse (MAFC or λ_C) exceedance (i.e., not the limit state intensity but the actual collapse rate, see Vamvatsikos *et al.* (Vamvatsikos et al., 2016) for further details) is unknown, the approach described in Vamvatsikos (Vamvatsikos, 2013) is adopted to compute λ_C based on the closed-form intensity-based formulation:

$$\lambda_C = \sqrt{p}k_0^{1-p}[H(\widehat{Sa}_{avg,C})]^p \exp\left[\frac{1}{2}pk_1^2\beta_C^2\right] \quad (13)$$

$$p = \frac{1}{1 + 2k_2{\beta_C}^2} \quad (14)$$

where $\widehat{Sa}_{avg,C}$ and β_C are the median collapse intensity and associated dispersion identified from the response estimation tool described previously in Figure 2.

2.5. Direct economic loss estimation

The direct economic loss is taken as the sum of three mutually exclusive, collectively exhaustive events, conditioned on a ground-motion intensity *im*: non-collapse requiring repair, non-collapse requiring demolition and total replacement due to collapse. Subsequently, the expected annual loss (EAL) of the building can be evaluated by integrating the vulnerability curves with the site hazard curve given by Equation 15.

$$EAL = \int E[L_T|IM = im]\left|\frac{dH(IM > im)}{dim}\right| dim \quad (15)$$

where the expected total economic loss term $E[L_T|IM = im]$ is defined via:

$$\begin{aligned} E[L_T|IM = im] = {} & E[L_T|NC \cap R, IM = im](1 - P[D|NC, IM = im])(1 - P[C|IM = im]) \\ & + E[L_T|NC \cap D]P[D|NC, IM = im](1 - P[C|IM = im]) + E[L_T|C]P[C|IM \\ & = im] \end{aligned} \quad (16)$$

where Equation 16 accounts for the probability of requiring demolition given non-collapse of the building or $P[D|NC, IM = im]$ due to the excessive RPSD; $E[L_T|NC \cap R, IM = im]$ is the expected repair at a given intensity *im* conditioned on non-collapse and the repairability of the building; $P[C|IM = im]$ is the collapse probability at an intensity *IM=im* and it is typically a lognormal cumulative distribution expressed in terms of the median collapse intensity and the associated dispersion due to record-to-record variability and other sources (e.g., modelling uncertainties); $E[L_T|C]$ is the expected loss given collapse or simply the total replacement cost; $E[L_T|NC \cap D]$ is the expected loss given no collapse and the non-repairability of the building, which is likely equal to $E[L_T|C]$. A simplified description to calculate the components of Equation 16 is presented in the following sub-sections.

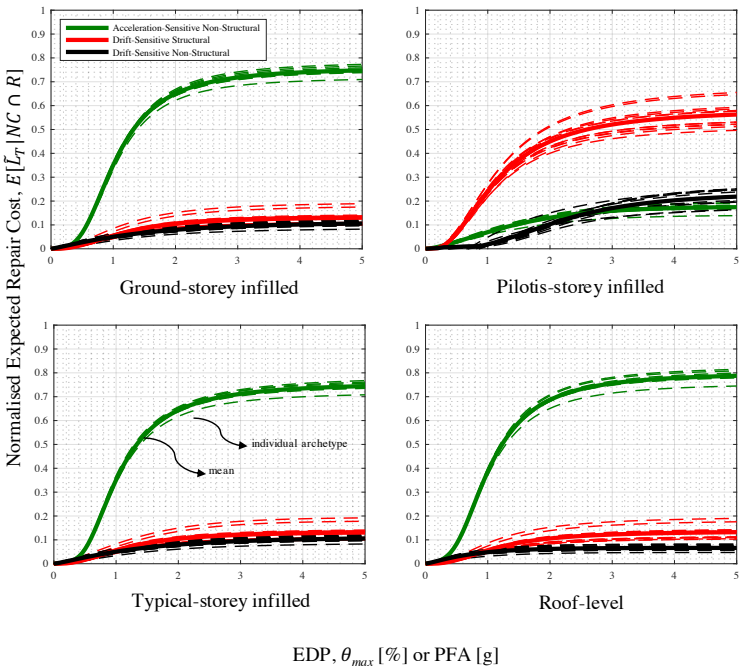

Figure 5: Generalised storey-loss functions for infilled RC storey typologies

2.5.1. Non-collapse: repairability

The term $E[L_T|NC \cap R, IM = im]$ of Equation 16 defines the expected losses sustained following an earthquake event with intensity *IM=im* that does not require demolition, but instead requires repair actions to be carried out. To estimate this, the generalised SLFs previously described by Nafeh and O'Reilly (Nafeh and O'Reilly, 2023) can be used to directly estimate the expected repair costs. As such, the user must:

a) Identify the most suitable SLF set from those available, or simply derive a set using the SLF generator proposed by Shahnazaryan *et al.* (2021);

b) For each separate performance group (PG), determine the expected loss ratio due to repair $E[L_T|NC \cap R, IM = im]_{PG,i}$ from SLFs using the relevant EDP from the previously estimated PSD or PFA demand profiles and SLF pair (Figure 5) at each intensity *im* and storey *i*;

c) Sum the contribution of each PG to the total repair costs at storey *i* as:

$$E[L_T|NC \cap R, IM = im]_i = \sum_{PG} E[L_T|NC \cap R, IM = im]_{PG,i} \quad (17)$$

d) Repeat the previous step for each storey *i*;

e) At each *im* level, the total expected repair cost for the entire building can be derived as:

$$E[L_T|NC \cap R, IM = im] = \sum_{i=1}^{N} E[L_T|NC, IM = im]_i \quad (18)$$

2.5.2.Non-collapse: demolition

The term $E[L_T|NC \cap D]P[D|NC, IM = im]$ of Equation 16 defines the expected losses due to demolition when a building possesses excessive permanent lateral deformation following an earthquake and repairability may no longer prove to be feasible. $E[L_T|NC \cap D]$ denotes the expected costs associated with demolition and $P[D|NC, IM = im]$ is the probability of requiring demolition. In most cases, the term $E[L_T|NC \cap D]$ is likely equal to the total replacement cost of the building. In *PB-Loss*, the probability of demolition is calculated using the residual drift fragility proposed by Ramirez and Miranda (2009). The probability that demolition would be required for a given value of RPSD is assumed to be lognormally distributed with a median of 1.5% and

dispersion of 0.3 as per Equation 19. In *PB-Loss*, the maximum value of the estimated RPSD along the height (from Equation 12) is used and a probability of demolition is obtained as per Figure 6.

$$P[D|NC, IM = im] = \Phi\left(\frac{\ln\left(RPSD/1.5\right)}{0.3}\right) \tag{19}$$

2.5.3. Collapse: total replacement

The term $E[L_T|C]P[C|IM = im]$ of Equation 16 defines the total expected replacement of the structure due to collapse where $E[L_T|C]$ corresponds to the expected cost associated with the total replacement of a given structure (i.e., debris removal and complete replacement) and $P[C|IM = im]$ is the probability the building collapsed. The collapse fragility function is expressed via a lognormal distribution as per Equation 20 where the median collapse intensity and associated dispersion, are retrieved from the response estimation tool and for each identified *im*, a collapse probability can be evaluated as per Figure 6.

$$P[C|IM = im] = \Phi\left(\frac{\ln\left(im/\widehat{Sa}_{avg,C}\right)}{\beta_C}\right) \tag{20}$$

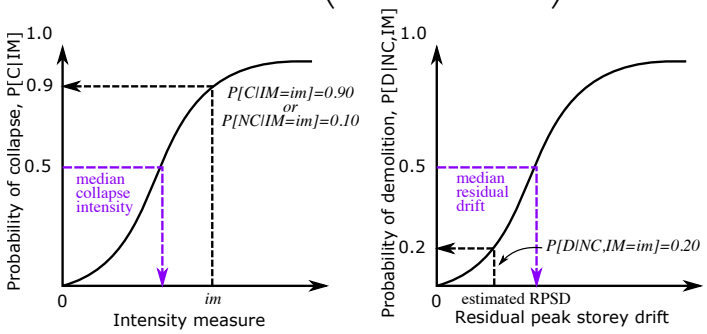

Figure 6: Example illustration of (left) collapse, P[C|IM=im], and (right) demolition, P[D|NC,IM=im], probability quantification

2.5.4. Expected annual loss calculation

The loss estimation of a case study building via *PB-Loss* concludes with the assembly of the loss curve, as illustrated in Figure 7. This relates the total expected loss (Equation 16) to the ground-shaking intensity sustained by a building at a particular site of interest. The EAL is then computed by integrating the loss curve via Equation 15. To this end, the following steps are implemented:

a) For each intensity *im*, plot the total expected loss $E[L_T|IM = im]$ versus *H*(*IM*);

b) An initial point is defined on the loss curve, namely the zero-loss (ZL) point, which represents the IM level where it is assumed that beyond this intensity, the losses are no longer non-negligible (i.e., $E[L_T|IM = im_{ZL}] = 0$). *H*(im_{ZL}) is assumed to be at a return period of 10 years, which is consistent with other simplified guidelines (Cosenza et al., 2018)

c) For collapse, the expected loss ratio is considered equal to be $E[L_T|C] = 1.0$ and the MAFC that describes its exceedance rate was previously quantified via Equation 13.

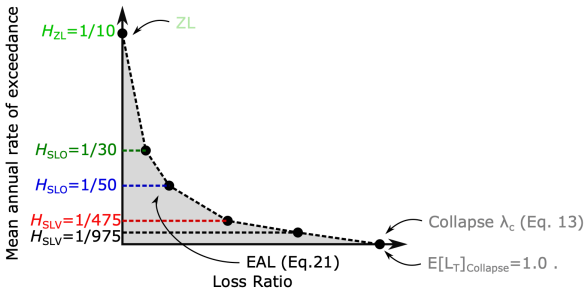

Figure 7: Assembling the loss curve

d) To compute the EAL, the user must then integrate the area under the loss curve (i.e., $E[L_T|IM = im]$ vs $H(IM)$) as shown in Figure 7. When a sufficient number of points have been established, the area can be evaluated using the trapezoidal rule as:

$$EAL = \lambda_c E[L_T|C] + \sum_{i=2}^{n} (\lambda_i - \lambda_{i-1}) \left[\frac{[E[L_T|im_i] - E[L_T|im_{i-1}]]}{2} \right] \quad (21)$$

where i=1 and i=n correspond to ZL and collapse, respectively; λ is the mean annual rate of exceedance. Here, five non-collapse intensities were considered but Equation 21 is generalisable to consider additional intensities depending on the user's preferences regarding the degree of acceptable accuracy-computational effort trade-off in numerical integration errors.

3. Performance comparison: expected annual losses

A performance assessment of the *PB-Loss* approach and the Italian guidelines for seismic risk classification of constructions methodology implemented in the Italian national guidelines for seismic risk classification was carried out. The outcome of the two methods, expressed in terms of the EAL, was compared to the results of the more rigorous component-based approach outlined in FEMA P-58. Seventy non-ductile infilled RC case study structures selected to be located in L'Aquila, Italy, were considered for the comparison, which are accessible at: https://github.com/gerardjoreilly/Infilled-RC-Building-Database. The building database consists of numerical building models developed in OpenSees and representative of non-ductile Italian construction practice adopted before the introduction of modern seismic guidelines. Details on the range of the parameters characterizing the database of infilled RC buildings used for the validation are provided in Table 3 (i.e. plan dimensions, storey height, infill thickness and mechanical properties, concrete strength, etc).

Table 3: Properties of analysed archetype numerical models

Number of stories	2-6 storeys
Storey height (m)	2.8 to 3.2
Floor Area (m2)	118 to 220
Column sections (cm)	20x20, 25x25, 30x30
Beam sections (cm)	50x30, 55x30, 30x70, 35x75
Longitudinal reinforcement ratios	Columns: 0.75-0.98%(ϕ16) Beams: 0.21-0.95% (ϕ14-ϕ16)
Material Characteristics	Smooth rebars (Aq42, σallowable=140 MPa); Deformed Rebars (FeB44k, σallowable =260 MPa); Concrete (20 - 25 MPa);
Infill typology and thickness (according to Hak et al. 2012)	Weak: 80mm Medium: 240mm Strong: 300mm

For the application of the component-based approach, multiple-stripe analyses (MSA) were carried out using hazard-consistent ground motion records to characterise the seismic response of the case study building population where Sa_{avg} was adopted as the IM. Hazard was characterised using the OpenQuake engine (Pagani et al., 2014) along with the 2013 Euro-Mediterranean seismic hazard model (ESHM13) (Woessner et

al., 2015). Ground motion records were selected from the NGA-W2 database using the conditional spectrum (Kohrangi et al., 2017) for Sa_{avg} and the geometric mean of the two components was considered for the selection. MSA was conducted for nine intensity measure levels corresponding to return periods of 22, 42, 72, 140, 224, 475, 975, 2475 and 4975 years to characterise the structural response from initial damage of the masonry infill panels right up to global structural collapse. The structural performance in terms of PSDs, PFAs and RPSDs was characterised at each IM level and served as input for the vulnerability component in the PACT tool. For the application of Italian guidelines for seismic risk classification of constructions concerning the estimation of the EAL values, the procedure outlined in Cosenza *et al.* (Cosenza et al., 2018) was adopted.

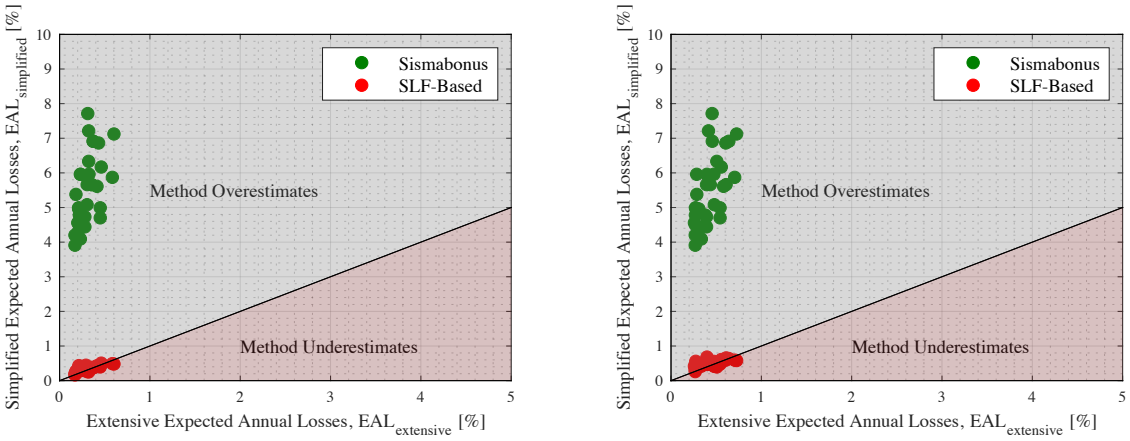

Figure 8: Comparison of simplified and extensive methodologies for seismic loss assessment applied to (a) gravity-load designed (pre-1970s) and (b) equivalent lateral-force (1970s-1980s buildings) designed non-ductile infilled RC frame buildings

Figure 8 illustrates the EAL values evaluated following the two simplified approaches. These values were compared to those obtained after carrying out extensive assessment using PACT; the details of which are omitted here for brevity, but are available in Nafeh and O'Reilly (2023). It was demonstrated that the approach in the Italian guidelines for seismic risk classification of constructions consistently yielded values which highly overestimated the EAL when compared to PACT. This difference is due to the simplifications in the approach adopted by the Italian guidelines for risk classification which were required for its integration with existing codes of practice, rendering it more accessible to practitioners. One of the main simplifications is the limit-state-to-loss ratios being fixed percentages of the total replacement cost, regardless of building typology or occupancy. This aspect was further investigated in O'Reilly *et al.* (2018) by comparing the expected loss ratio at each limit-state from detailed analysis with the fixed expected loss ratios outlined in the guidelines. It was shown that the expected loss ratios at each limit state computed using detailed analysis were much lower than the fixed values specified in the guidelines, explaining the difference in magnitude between the EAL values observed in Figure 8. Moreover, it is evident through the illustrative comparison presented in Figure 8 that the *PB-Loss* approach yielded relatively good estimates when compared to the extensive methodology. This is due to the adaptability of the proposed storey loss functions in characterising economic losses closely related to the structural response expressed in terms of the seismic demand (i.e., PSD and PFA). Based on these promising results regarding the accuracy of SLF-based loss assessment, the integration of such simplified tools for the response estimation of structures in terms of demand parameters (i.e., PSDs and PFAs) is appealing to analysts. This integration could encourage a more demand-based estimation of the associated losses at different levels of ground-shaking intensity. This is contrary to pre-calibrated and fixed loss ratios currently adopted in the Italian guidelines for seismic risk classification of constructions whose applicability may be limited to the cases for which they were developed. However, if the approach can be adapted to align more closely with detailed component-based analysis using the same source data, the method can be more generally applied as it follows the underlying physics of loss accumulation in structures more closely.

4. Conclusions

In recent years, seismic risk assessment has undergone a paradigm shift from its traditional focus primarily on building performance to incorporate broader issues associated with economic losses and ensuring life safety. Furthermore, the trade-off between simplicity and accuracy remains an open challenge for researchers to provide practitioners and decision-makers with simplified tools to characterise the seismic performance of structures accurately. Additionally, evaluating the direct monetary losses sustained in seismic events, through metrics such as the expected annual losses (EAL), for example, is paramount for existing reinforced concrete (RC) buildings with masonry infills due to their prevalence in regional building stocks. In loss-based analyses, the component-based approach is heavily dependent on the results of computationally expensive and time-consuming non-linear time-history analyses (NLTHA). This has been further demonstrated through the introduction of seismic risk guidelines in Italy. These guidelines, such as Italian guidelines for seismic risk classification of constructions, offer a simple and practice-oriented solution which has undoubtedly aided its widespread application. However, further scrutiny has shown that with respect to the more exhaustive NLTHA-based component-based methods, The Italian guidelines for seismic risk classification may possess some limitations and drawbacks that can be improved in future revisions. This was seen in this study for the case of non-ductile infilled RC buildings in the loss estimates that significantly differed to those obtained from the more rigorous approach described in FEMA P-58. Thus, a solution in the form of a pushover-based seismic loss assessment method, termed *PB-Loss,* was discussed. *PB-Loss* highlights the benefit of integrating generalised storey-loss functions in future revisions of national guidelines on risk classification and loss assessment of buildings. The performance of the proposed *PB-Loss* methodology in accurately evaluating the direct economic losses due to ground-shaking was validated within a comparative case study application. The results highlighted the reliability and consistency of the proposed approach when compared to the results of an extensive analysis performed in PACT on numerical models with hazard-consistent ground motions. Some of the work and tools developed in recent years that would facilitate such usage were described. Again, within the scope of providing a practitioner-friendly tool that could help build a more robust future revision, some of the recent work done in this regard was described.

5. Acknowledgements

The work presented in this paper has been developed within the framework of the project "Dipartimenti di Eccellenza 2023-2027", funded by the Italian Ministry of Education, University and Research at IUSS Pavia.

6. References

CNR (2014). Istruzioni per la Valutazione Affidabilistica della Sicurezza Sismica di Edifici Esistenti.

Cornell C.A., Krawinkler H. (2000). Progress and Challenges in Seismic Performance Assessment, PEER Center News, 3(2): 1–4.

Cosenza E., Del Vecchio C., Di Ludovico M., Dolce M., Moroni C., Prota A., Renzi E. (2018). The Italian guidelines for seismic risk classification of constructions: technical principles and validation, Bulletin of Earthquake Engineering, 16(12): 5905–5935.

Eads L., Miranda E., Lignos D.G. (2015). Average spectral acceleration as an intensity measure for collapse risk assessment, Earthquake Engineering and Structural Dynamics, 44(12): 2057–2073.

FEMA (2012a). FEMA P58-1. Seismic Performance Assessment of Buildings: Volume 1 - Methodology (P-58-1). vol. 1. Washington, DC.

FEMA (2012b). Seismic Performance Assessment of Buildings Volume 1 – Methodology. FEMA P-58-1, Federal Emergency Management Agency, 1(August): 278.

Kohrangi M., Bazzurro P., Vamvatsikos D., Spillatura A. (2017). Conditional spectrum-based ground motion record selection using average spectral acceleration, Earthquake Engineering and Structural Dynamics, 46(10): 1667–1685.

Krawinkler H., Miranda E. (2004). Performance-based earthquake engineering In: Y. Bozorgnia and V. V. Bertero, eds. Earthquake engineering: From engineering seismology to performance-based engineering. Boca Raton, FL: CRC Press.

Ministero delle Infrastrutture e dei Trasporti (2017). Sismabonus: Decreto Ministeriale 58/2017

Muho E. V, Pian C., Qian J., Shadabfar M., Beskos D.E. (2021). Deformation-dependent peak floor acceleration for the performance-based design of nonstructural elements attached to R/C structures, Earthquake Spectra, 37(2): 1035–1055.

Nafeh A.M.B., O'Reilly G.J. (2023). Simplified pushover-based seismic risk assessment methodology for existing infilled frame structures, Bulletin of Earthquake Engineering, 21(4): 2337–2368.

Nafeh A.M.B., O'Reilly G.J. (2022). Unbiased simplified seismic fragility estimation of non-ductile infilled RC structures, Soil Dynamics and Earthquake Engineering, 157: 107253.

Nafeh, O'Reilly G.J. (2023). Simplified pushover-based seismic loss assessment for existing infilled frame structures, Bulletin of Earthquake Engineering,.

NTC (2018). Norme Tecniche Per Le Costruzioni Rome, Italy.

O'Reilly G.J. (2021). Limitations of Sa(T 1) as an intensity measure when assessing non-ductile infilled RC frame structures, Bulletin of Earthquake Engineering, 19(6): 2389–2417.

O'Reilly G.J., Nafeh A.M.B. (2021). Infilled-RC-Building-Response-Estimation, GitHub Repository,.

O'Reilly G.J., Perrone D., Fox M., Monteiro R., Filiatrault A. (2018). Seismic assessment and loss estimation of existing school buildings in Italy, Engineering Structures, 168: 142–162.

Pagani M., Monelli D., Weatherill G., Danciu L., Crowley H., Silva V., Henshaw P., Butler L., Nastasi M., Panzeri L., Simionato M., Vigano D. (2014). Openquake engine: An open hazard (and risk) software for the global earthquake model, Seismological Research Letters, 85(3): 692–702.

Ramirez C.M., Miranda E. (2009). Building Specific Loss Estimation Methods & Tools for Simplified Performance Based Earthquake Engineering, Blume Report No. 171,.

Shahnazaryan D., O'Reilly G.J. (2023). Fitting improved hazard models for SAC/FEMA-compatible seismic analysis In: 14th International Conference on Applications of Statistics and Probability in Civil Engineering, ICASP14. Dublin, Ireland.

Shahnazaryan D., O'Reilly G.J., Monteiro R. (2021). Story loss functions for seismic design and assessment: Development of tools and application, Earthquake Spectra, 37(4): 2813–2839.

Silva A., Castro J.M., Monteiro R. (2020). A rational approach to the conversion of FEMA P-58 seismic repair costs to Europe, Earthquake Spectra, 36(3): 1607–1618.

Vamvatsikos D. (2013). Derivation of new SAC/FEMA performance evaluation solutions with second-order hazard approximation, Earthquake Engineering & Structural Dynamics, 42(8): 1171–1188.

Vamvatsikos D., Kazantzi A.K., Aschheim M.A. (2016). Performance-Based Seismic Design: Avant-Garde and Code-Compatible Approaches, ASCE-ASME Journal of Risk and Uncertainty in Engineering Systems, Part A: Civil Engineering, 2(2).

Del Vecchio C., Di Ludovico M., Pampanin S., Prota A. (2018). Repair Costs of Existing RC Buildings Damaged by the L'Aquila Earthquake and Comparison with FEMA P-58 Predictions, Earthquake Spectra, 34(1): 237–263.

Woessner J., Laurentiu D., Giardini D., Crowley H., Cotton F., Grünthal G., Valensise G., Arvidsson R., Basili R., Demircioglu M.B., Hiemer S., Meletti C., Musson R.W., Rovida A.N., Sesetyan K., Stucchi M. (2015). The 2013 European Seismic Hazard Model: key components and results, Bulletin of Earthquake Engineering, 13(12): 3553–3596.